Biological Psychology 82 (2009) 82–88

Contents lists available at ScienceDirect

Biological Psychology

journal homepage: www.elsevier.com/locate/biopsycho

Breathing frequency bias in fractal analysis of heart rate variability

Pandelis Perakakis [a,*], Michael Taylor [b], Eduardo Martinez-Nieto [a], Ioanna Revithi [c], Jaime Vila [a]

[a] Department of Personality, Evaluation and Psychological Treatment, Faculty of Psychology, University of Granada, Campus Cartuja, 18071 Granada, Spain
[b] Institute for Space Applications and Remote Sencing, National Observatory of Athens, Vas. Pavlou & I. Metaxa, 15236 Penteli, Greece
[c] Faculty of Psychology, Aristo tle University of Thessaloniki, Thessaloniki, Greece

ARTICLE INFO

Article history:
Received 1 January 2009
Accepted 16 June 2009
Available online 25 June 2009

Keywords:
Heart rate variability
Detrended Fluctuation Analysis
Fractal correlations
Respiratory sinus arrhythmia
Paced breathing

ABSTRACT

Detrended Fluctuation Analysis (DFA) is an algorithm widely used to determine fractal long-range correlations in physiological signals. Its application to heart rate variability (HRV) has proven useful in distinguishing healthy subjects from patients with cardiovascular disease. In this study we examined the effect of respiratory sinus arrhythmia (RSA) on the performance of DFA applied to HRV. Predictions based on a mathematical model were compared with those obtained from a sample of 14 normal subjects at three breathing frequencies: 0.1 Hz, 0.2 Hz and 0.25 Hz. Results revealed that: (1) the periodical properties of RSA produce a change of the correlation exponent in HRV at a scale corresponding to the respiratory period, (2) the short-term DFA exponent is significantly reduced when breathing frequency rises from 0.1 Hz to 0.2 Hz. These findings raise important methodological questions regarding the application of fractal measures to short-term HRV.

1. Introduction

Extraordinary structural and functional complexity is a defining characteristic of living organisms. This complexity gives rise to physiological signals that exhibit interesting properties such as scale invariance and long-term correlations. Statistical physics has only recently began to develop the appropriate mathematical tools to understand and quantify these properties present in a wide variety of biological, physical and social complex systems (Stanley et al., 1996, 1999, 2000).

Generally, signals exhibiting fluctuations whose distribution obeys a power law over a broad range of frequencies are scale invariant and usually referred to as fractal (Mandelbrot, 1983). Fluctuations (F) in these signals can be expressed as a function of the time interval (n) over which they are observed according to the formula:

$$F(n) = pn^{\alpha} \quad (1)$$

where p is a constant of proportionality and α is a scaling exponent that depends on the signal correlation properties. The special case of $\alpha = 1$ is frequently observed in nature and is often called $1/f$ *noise*. Signals exhibiting $1/f$ noise are characteristic of complex dynamical systems, composed of multiple interconnected elements and functioning in far from equilibrium conditions (Bak et al., 1987). These systems demonstrate optimal stability, information transmission, informational storage and computational power (Beggs, 2008). Hence, $1/f$ fluctuations are commonly considered as an indicator of the efficacy and adaptability of the system that produces them (Jensen, 1998).

HRV has been extensively studied by psychophysiologists as an indirect index of autonomic function in health and disease (Camm et al., 1996; Berntson et al., 1997). Common HRV measures include time and frequency domain metrics. Time domain measures calculate the overall variance or the variability between successive interbeat intervals (IBI) using linear statistics. Frequency domain measures assess the variability of the power spectrum in predetermined frequency bands. The rationale for the use of all these different HRV methods in psychophysiological research is to identify and measure characteristic components of heart rate fluctuations that can be associated with specific physiological control mechanisms such as respiratory sinus arrhythmia (RSA) and baroreflex activity (Allen et al., 2007).

The power spectrum of 24-h heart rate records, however, also reveals that the proportion of the signal in different frequency bands is inversely proportional to the frequency over a wide range of scales (Kobayashi and Musha, 1982; Saul et al., 1988). This evidence of fractal $1/f$ noise in heart rate fluctuations may imply that cardiac regulation mechanisms are organized in a critical state that allows maximum adaptability to internal and external stimulation (Stanley et al., 2000). More detailed aspects of this organization can be assessed by algorithms that preserve the temporal information present in the signal. DFA is one of the algorithms that has been widely used to quantify IBI correlation properties as a complementary measure to more traditional HRV indices (Eke et al., 2002; Huikuri et al., 2003). Initial results indicate that healthy HRV is characterized by $1/f$ scaling, while deviations

* Corresponding author.
E-mail address: peraka@ugr.es (P. Perakakis).

0301-0511/$ – see front matter © 2009 Elsevier B.V. All rights reserved.
doi:10.1016/j.biopsycho.2009.06.004

from this value are associated with aging and disease (Peng et al., 1993; Goldberger et al., 2002).

The aim of this study is twofold. Firstly, to introduce in a brief and concise manner the DFA as an HRV measure that is rarely encountered in the biopsychological literature. We believe that scaling analysis of cardiac dynamics can be used effectively to probe how complexity is generated in the cardiovascular system and also to improve our understanding of how the heart responds to internal and external stimulation. With this in mind, in Section 4 we include some specific suggestions for further research. Our second objective is to call attention to an important methodological issue in the fractal analysis of short-term HRV that has not been properly addressed in the literature. In our concluding remarks we will articulate our opinion regarding the delicate issue of applying the DFA on short-term HRV.

1.1. Detrended Fluctuation Analysis

DFA was introduced by Peng (Peng et al., 1995) and has been successfully used to quantify correlation properties in nonstationary time series derived from biological, physical, and social systems. It has been applied in various research fields including economics (Weron, 2002), climate temperature fluctuations (Vjushin et al., 2002), DNA (Buldyrev et al., 1998), neural networks (Stam et al., 2005), and cardiac dynamics (Peng et al., 1995). In the application of DFA to HRV, the IBI series B (of length N) is first integrated in order to calculate the sum of the differences between the ith interbeat interval $B(i)$ and the mean interbeat interval B_{ave} : $y(k) = \sum_{i=1}^{k}[B(i) - B_{\text{ave}}]$. Next, the integrated series $y(k)$ is divided into boxes of equal length n (measured in number of beats). Each box is subsequently detrended by subtracting a least-squares linear fit, denoted $y_n(k)$. The root-mean-square (RMS) F of this integrated and detrended time series is calculated by

$$F(n) = \sqrt{\frac{1}{N}\sum_{k=1}^{N}[y(k) - y_n(k)]^2} \quad (2)$$

This algorithm is repeated over a range of box sizes to provide a relationship between the mean fluctuation $F(n)$ as a function of box size n. Normally, $F(n)$ will increase as box size n becomes larger. According to Eq. (1), a linear relationship on a log–log graph indicates the presence of scaling characterized by the scaling exponent α. For uncorrelated time series (white noise), the integrated $y(k)$ is a random walk that yields an exponent of $\alpha = 0.5$. A scaling exponent $\alpha > 0.5$ indicates the presence of correlations in the original series such that a large IBI is more likely to be followed by another large interval, while $0 < \alpha < 0.5$ indicates anti-correlations such that large and small IBI values are more likely to alternate. The special case $\alpha = 1.5$ is obtained by the integration of highly correlated *Brown* noise and $\alpha = 1$ corresponds to $1/f$ noise which can be interpreted as a balance between the complete step-by-step unpredictability of random signals and highly correlated Brownian noise (Peng et al., 1992).

1.2. Application to IBI records

Peng et al. (Peng et al., 1995) applied the DFA algorithm to 24-h IBI records obtained from healthy subjects and patients with congestive heart failure, revealing two distinct scaling regions for both groups: one corresponding to short-term variability (smaller box sizes) and the other associated with long-term variability (larger box sizes). Therefore, two different scaling exponents were obtained: a short-term exponent for $4 \leq n \leq 16$ referred to as α_1 and a long-term exponent for $n \geq 16$ referred to as α_2.

Fig. 1 plots $\log F(n)$ against $\log n$ (which we will refer to as the DFA plot) for two subjects from the same database, which is freely

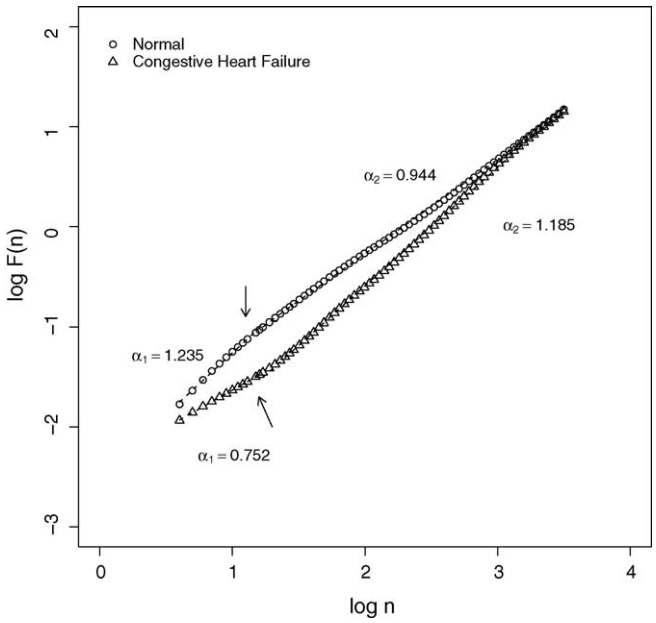

Fig. 1. Plot of $\log F(n)$ vs. $\log n$ from a healthy subject (circles) and from a subject with congestive heart failure (triangles). Arrows indicate crossovers that divide the DFA plot into two distinct scaling regions.

available from the Physionet website (Goldberger et al., 2000). It shows the two distinct scaling regions and their corresponding slopes. The arrows indicate the box size where the scaling changes (the crossover point). In healthy subjects, $1/f$ noise represented by $\alpha_2 \approx 1$ is exhibited over a broad range of time scales from mid to low frequencies (from $n = 16$ to 3400). Stronger correlations are found at higher frequencies (from $n = 4$ to 16), reflected by $\alpha_1 > 1$. In patients with congestive heart disease, long-term variability loses its fractal $1/f$ properties ($\alpha_2 > 1$), while short-term variability approximates uncorrelated randomness ($\alpha_1 \approx 0.5$).

1.3. Effects of sinusoidal trends on DFA

As noted above, scaling behavior is not constant throughout the IBI series, with crossovers occurring at the changeover from one RMS fluctuation power law to another. A crossover can arise either from a change in intrinsic IBI correlation properties or from external trends in the data (Peng et al., 1995). Therefore, a correct interpretation of the scaling exponent is necessary to distinguish between intrinsic heart rate fluctuations and trend-like fluctuations arising from other systematic effects. Distinctions of this kind are relevant because strong trends in the data can lead to a false detection of long-range correlations if DFA results are not carefully interpreted (Kantelhardt et al., 2001; Hu et al., 2001).

The DFA algorithm is capable of identifying and removing both linear and higher-order polynomial trends and avoids the spurious detection of apparent long-range correlations (Kantelhardt et al., 2001). However, this is not the case for exponential or sinusoidal trends (Xu et al., 2008; Nagarajan and Kavasseri, 2005). In Fig. 2 we present the DFA plot of correlated noise with scaling exponent $\alpha = 0.8$, superimposed by a sinusoidal trend with period $T = 15$ samples. The same graph also includes the DFA plot for the noise and sinusoidal trend separately. Constant scaling is observed with $\alpha \approx 0.8$ for the noise. However, the sinusoidal trend shows a clear crossover n_x, dividing $F(n)$ into two very distinct scaling regions. Hu et al. (Hu et al., 2001) showed that this crossover is found at a scale corresponding to the period of the sinusoid and is independent of its amplitude. For $n < n_x$, integration of the sinusoid produces a quadratic background that is not filtered

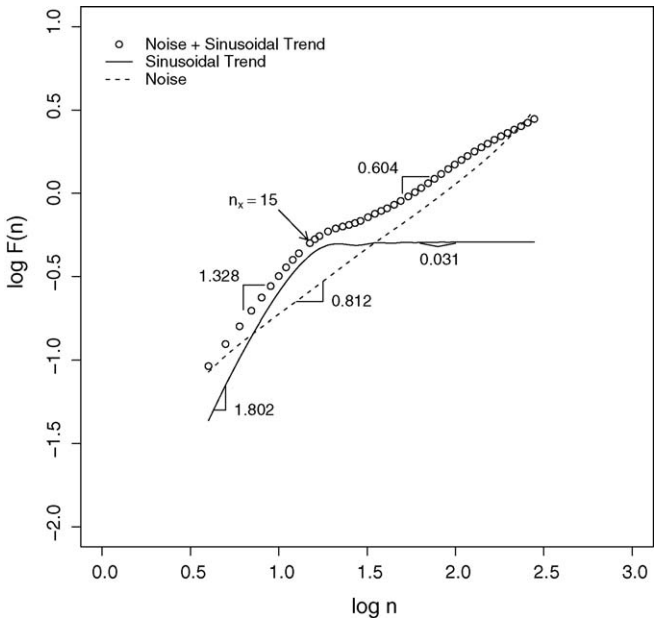

Fig. 2. Crossover behavior of the fluctuation function $F(n)$ for correlated noise superimposed with a sinusoidal function with period $T = 15$. The fluctuation function for noise and the fluctuation function for the sinusoidal trend are shown separately for comparison. The arrow indicates the scaling crossover at scale $n_x = 15$ ($\log_{10}(15) = 1.1761$) corresponding to the period of the sinusoidal trend.

out by the linear detrending of the DFA algorithm. Thus, in this region, $F(n)$ is sensitive to the quadratic trend and the slope of $\log F(n)$ increases steeply as box sizes become larger. For $n > n_x$, the box size is large enough to contain a whole cycle and, at these scales, fluctuations associated with local gradient changes along the sine wave are not detectable. Hence, $F(n)$ no longer depends on n, leading to a flattening of the DFA plot.

The DFA plot of the noise and sinusoidal trend shows a scaling behavior produced by competition between the two signals. To explain this effect analytically, Hu et al. demonstrated that for any two independent signals (s1 and s2), the RMS fluctuation function for a third signal resulting from their superposition is given by

$$[F_{s1s2}(n)]^2 = [F_{s1}(n)]^2 + [F_{s2}(n)]^2 \quad (3)$$

This "superposition rule" allows a mathematical description of how the competition between the contribution of the fluctuation function of the correlated noise $F_{\text{noise}}(n)$ and the fluctuation function of the sinusoidal trend $F_{\text{sinus}}(n)$ at different scales n leads to the appearance of scaling crossovers (Hu et al., 2001). For $n < n_x$, $F_{\text{sinus}}(n)$ is dominant, leading to a high DFA exponent ($\alpha = 1.328$). For $n > n_x$, however, the contribution of $F_{\text{noise}}(n)$increases, leading to a gradual decrease in the DFA exponent.

At high frequencies, HRV is dominated by rather smooth rhythmical oscillations associated with breathing (RSA) (Berntson et al., 1993). In the IBI power spectrum of healthy individuals at rest, RSA is evidenced as a clearly distinct peak at the respiratory frequency (Kleiger et al., 2005). We assumed therefore that RSA would produce a scaling behavior of short-term HRV similar to that of a sinusoidal trend superimposed on correlated noise. It can be argued that RSA is not always adequately approximated by a sinusoid since there is significant variability in the inspiration/expiration ratio (Boiten et al., 1994). However, it is clear from our previous analysis that the strongly correlated region at scales smaller than the crossover is caused by increases in the fluctuation function $F(n)$ that are mostly influenced by the local constant gradient of the periodic signal and not by the exact form of the sinusoidal function.

To experimentally test the above assumption, we designed a study to explore the effects of RSA on the DFA of IBI series and compared them with those observed when a sinusoidal trend is superimposed on a correlated noise. We proposed two hypotheses:

1. Respiratory oscillations produce a crossover that divides the $\log F(n)$ plot into two significantly different scaling regions.
2. Changes in breathing frequency $B(f)$ affect the location of the crossover, producing predictable alterations in the value of the short-term scaling exponent obtained by the DFA algorithm.

2. Method

The hypotheses were tested in a physiological experiment involving 14 university students (6 males) aged 20–23 years (mean = 21.79 ± 0.89 years), who were instructed to breathe at specific frequencies (0.1 Hz, 0.2 Hz and 0.25 Hz) following a sinusoidal tone heard on headphones. Each breathing condition lasted for 5 min and was preceded by a training session to ensure participants were able to perform the task without difficulties. At the end of each breathing condition, subjects were given the chance to have a short break to relax before commencing with the next respiratory pattern. Prior to the three breathing conditions, that were always performed in the same order, we also recorded 5 min of spontaneous breathing. During each experimental session, continuous ECG (at a sample rate of 1000 Hz) was recorded by a Powerlab data acquisition system (4/25 T). R-wave detection and artifact correction were performed with *Ecglab* (Carvalho et al., 2002).

The location of the crossover in the plot of $\log F(n)$ was calculated for each subject using the relation,

$$n_x = \frac{T}{\langle \text{IBI} \rangle} \quad (4)$$

where T is the respiratory period and $\langle \text{IBI} \rangle$ is the average heart period calculated over the entire 5-min breathing period. Eq. (4) therefore represents the box size (number of beats) that contains a complete respiratory cycle dependent on the average interbeat interval of each subject.

KARDIA (Perakakis et al., 2008), a Matlab Toolbox designed for IBI data analysis was used to obtain scaling exponents, power spectrum graphs and DFA plots. Spectral analysis was performed after interpolating the IBI series with cubic splines at 2 Hz. The interpolated series was subsequently detrended, by removing the best straight-line fit and multiplied by a Hanning window function. The discrete Fourier transform (DFT) was calculated by means of fast Fourier transform with 512 points. Finally, the Fourier power spectral density was obtained from the squared absolute value of the DFT, multiplied by the sampling period and divided by the number of samples in the signal. The short-term DFA exponent was calculated after implementing a first-order DFA algorithm (as described in Section 1.2) for box sizes ranging from 4 to 16 beats according to the original suggestion by Peng et al. (Peng et al., 1995). To avoid ambiguity, the designation α_{4-16} was selected for this short-term DFA exponent, which is usually denoted α_1 in the literature, because we will use the terms α_1 and α_2 to refer to the exponents of the two scaling regions defined by the respiratory crossover. Statistical significance was tested by paired Student's t-test.

3. Results

Visual inspection of the power spectra revealed distinctive peaks at the expected frequencies (0.1 Hz, 0.2 Hz and 0.25 Hz) for all subjects and conditions. This was used as a measure to assure that participants had followed the instructions correctly producing the desired respiratory patterns. Table 1 shows the average IBI values, the predicted box size at which the respiratory crossover should appear according to Eq. (4), the scaling exponent for the two regions defined by the crossover, and the scaling exponent obtained for $4 \leq n \leq 16$.

To test our first hypothesis, we compared the scaling exponents obtained for the regions before and after the location of the respiratory crossover (α_1 and α_2 respectively). In all breathing conditions, the two exponents were significantly different, confirming the hypothesis. In every case, α_1 was significantly higher than α_2 ($Bf = 0.1$ Hz: $t_{13} = 23.21$, $p < 0.001$; $Bf = 0.2$ Hz: $t_{13} = 16.65$, $p < 0.001$; $Bf = 0.25$ Hz: $t_6 = 7.77$, $p < 0.001$ [1]).

[1] For $Bf = 0.25$ Hz, the α_1 exponent could only be calculated for the cases in which $n_x > 4$.

Table 1
Results for 14 subjects breathing at frequencies of 0.1 Hz, 0.2 Hz, and 0.25 Hz

Subjects	0.1 Hz					0.2 Hz					0.25 Hz				
	IBI	n_x	α_1	α_2	α_{4-16}	IBI	n_x	α_1	α_2	α_{4-16}	IBI	n_x	α_1	α_2	α_{4-16}
1	823	12	1.628	0.528	1.41	818	6	1.496	0.668	0.86	831	4		0.881	0.92
2	945	10	1.636	0.364	1.23	958	5	1.456	0.493	0.64	983	4		0.399	0.44
3	785	12	1.594	0.722	1.42	763	6	1.336	0.848	0.98	770	5	1.521	1.07	1.13
4	801	12	1.469	0.562	1.29	810	6	1.429	0.589	0.8	852	4		0.482	0.55
5	820	12	1.52	0.534	1.33	818	6	1.4	0.285	0.58	808	4		0.599	0.66
6	917	10	1.678	0.428	1.28	913	5	1.582	0.822	0.95	908	4		0.845	0.88
7	808	12	1.655	0.545	1.44	813	6	1.515	0.365	0.67	817	4		0.812	0.87
8	734	13	1.552	0.65	1.43	714	7	1.426	0.629	0.89	714	5	1.642	1.222	1.29
9	763	13	1.597	0.68	1.46	751	6	1.677	1.086	1.24	733	5	1.736	1.235	1.32
10	858	11	1.655	0.503	1.36	848	5	1.518	0.521	0.71	859	4		0.768	0.82
11	727	13	1.51	0.679	1.4	733	6	1.421	0.345	0.67	759	5	1.222	0.489	0.59
12	776	12	1.387	0.593	1.24	724	6	1.506	0.426	0.74	727	5	1.5	0.472	0.63
13	759	13	1.518	0.569	1.39	735	6	1.543	0.427	0.74	751	5	1.442	0.626	0.75
14	765	13	1.349	0.537	1.24	723	6	1.577	0.714	0.96	775	5	1.536	0.932	1.03
Mean			1.553	0.564	1.351			1.492	0.587	0.816			1.514	0.774	0.849

IBI is the average cardiac interbeat interval, n_x is the predicted scale of the respiratory crossover, α_1 and α_2 are the exponents for the two scaling regions defined by the crossover, and α_{4-16} is the exponent for the region from 4 to 16 beats. There are data gaps at 0.25 Hz due to the small value of n_x in the fast breathing condition.

Our second hypothesis was tested by examining the effect of breathing frequency on the α_{4-16} exponent. We found that α_{4-16} was significantly reduced when the breathing frequency was increased from 0.1 Hz to 0.2 Hz ($t_{13} = 11.59$, $p < 0.001$). The comparison of α_{4-16} at 0.2 Hz and 0.25 Hz revealed no significant differences ($p = 0.487$). The high α_1 exponents in all breathing conditions are illustrated in the DFA plots for one subject (number 12) in Fig. 3. We note that $F(n)$ behavior strongly resembles the simulated data shown in Fig. 2.

In order to show that similar scaling behavior is observed during relaxed normal breathing, in Fig. 4 we compare DFA plots for three subjects during the spontaneous breathing session. Although RSA is not restricted to a narrow frequency band (as in paced breathing paradigms), it is evident that faster breathing frequencies produce a respiratory crossover at smaller scales. According to our prediction, slopes are always higher to the left of the crossover.

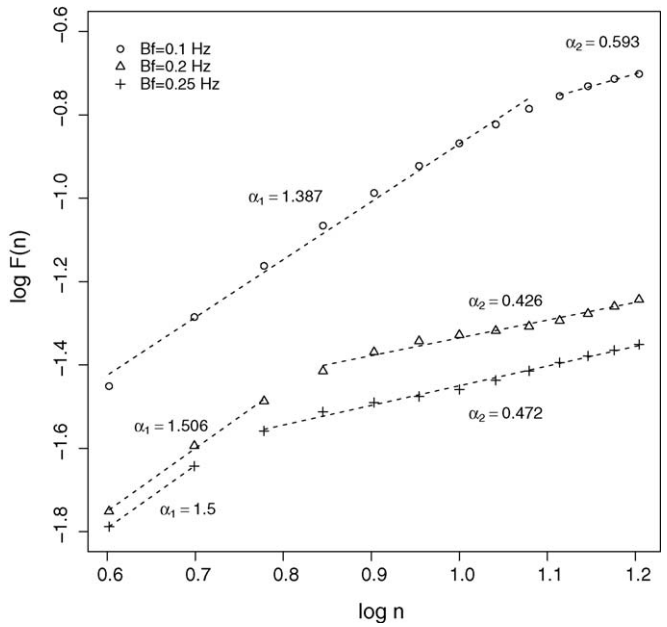

Fig. 3. Crossover behavior of the $F(n)$ function at different respiratory frequencies in one subject. Changes in scaling exponents indicate the location of the crossover. The crossover occurs at smaller scales as breathing becomes more rapid.

4. Discussion

In the original article introducing the DFA algorithm, Peng et al. noted that the high α_{4-16} exponents obtained from healthy subjects are: "... probably due to the fact that on very short time scales, the physiologic interbeat interval fluctuation is dominated by the relatively smooth heartbeat oscillation associated with respiration ...(Peng et al., 1995). The only systematic study on the effects of breathing frequency on the DFA short-term exponent reported that a reduction in the respiration rate from 15 breaths/min to 6 breaths/min increased the scaling exponent from 0.83 ± 0.25 to 1.18 ± 0.27 (Penttila et al., 2003). However, the authors offered no explanation for this effect.

Our study confirms the original suggestion by Peng et al. (Peng et al., 1995) that the crossover at scales close to the respiratory period is caused by periodic breathing oscillations. As shown in Section 1.3, this scaling behavior is similar in signals produced by the superposition of simulated correlated noise and sinusoidal trends. The superposition rule described by Eq. (3) explains the appearance of changes in scaling as a result of the competing contributions of the two signals at different time scales. Although, in the case of real IBI data we do not have independent signals, the principle of competing contributions can still be used to explain the scaling behavior of the $F(n)$ function. At short time scales (high frequencies), RSA is the dominant contribution in the IBI signal and $F(n)$ follows a constant local gradient with increasing n, leading to high scaling exponents. However, at scales longer than the respiratory crossover (given by Eq. (4)), box sizes contain a complete respiratory cycle and RSA no longer contributes to the increases in $F(n)$ with increasing box size.

The results also explain the effects of breathing frequency alterations on estimations of the short-term DFA scaling exponent. In accordance with our second hypothesis, we showed that the changes in $F(n)$ scaling caused by changes in respiratory period, affected the scaling exponent α_{4-16}, which is usually considered to account for HRV short-term correlations. We found that α_{4-16} was significantly higher in the slow breathing condition when the α_1 exponent extended over a time scale range of 4 to approximately 12 beats, exerting a strong influence on the value of the α_{4-16} exponent. Conversely, the α_1 exponent extended over a shorter time scale range in the fast breathing condition and α_{4-16} was closer to α_2.

4.1. Re-interpreting results of previous studies

Our findings have important methodological implications for the interpretation of previous reports. The short-term DFA

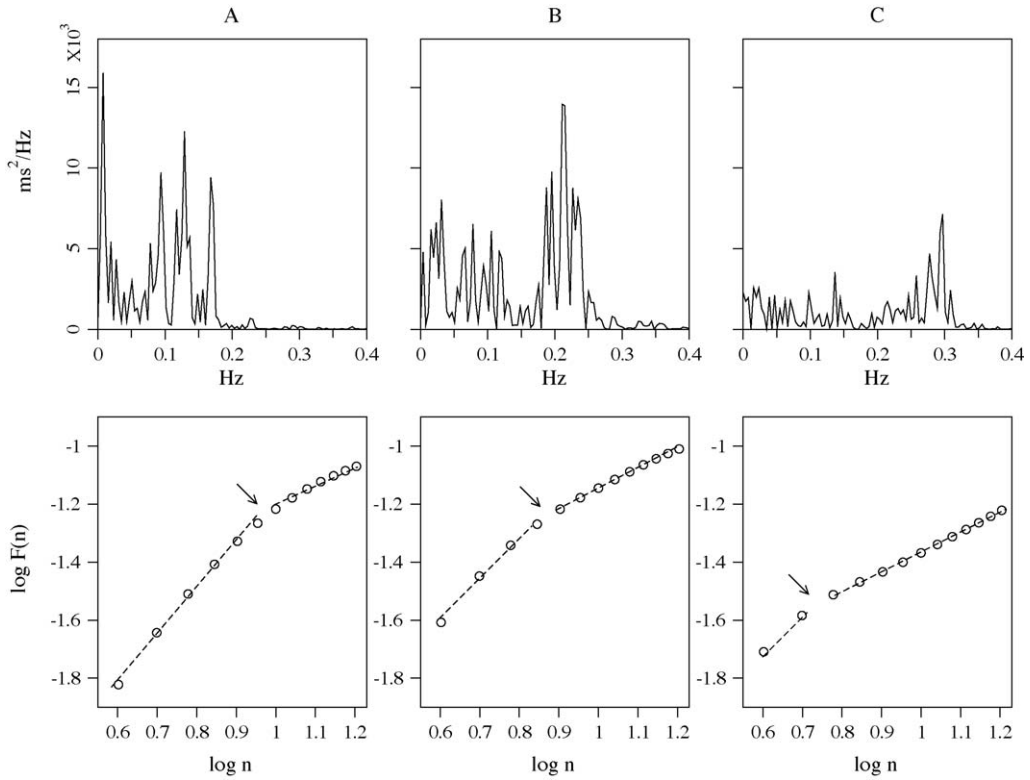

Fig. 4. Crossover behavior of the $F(n)$ function in three subjects (A–C) during spontaneous breathing. In the top row we observe a broad-band RSA at progressively faster frequencies as we move from subject A to subject C. Arrows on the DFA plots in the second row indicate scaling crossovers that are encountered at smaller scales for faster breathing frequencies.

exponent has proven to be a more accurate predictor of mortality in patients with depressed left ventricular function after an acute myocardial infarction in comparison to the more common HRV measures (Stein et al., 2008). Thus, reduced α_{4-16} predicted both arrhythmic and nonarrhythmic cardiac death (Huikuri et al., 2000). Other studies showed that α_{4-16} was reduced in patients with dilated cardiomyopathy (Mahon et al., 2002; Voss et al., 2007), and that reductions in the short-term DFA exponent are observed before the spontaneous onset of paroxysmal atrial fibrillation episodes (Vikman et al., 1999).

In our study, however, we have shown that changes in breathing frequency produce significant alterations in the short-term DFA exponent that were related to effects of RSA behaving as a sinusoidal trend rather than to autonomic cardiac control. We also predicted and confirmed the exact direction of these alterations as a function of the breathing frequency and heart rate. In general, slow periodic breathing tends to increase the scaling exponent, while faster breathing significantly reduces it. Therefore, it is essential to consider both respiration and heart rate in order to correctly interpret short-term HRV scaling behavior. For example, faster and more irregular breathing (implying hyperventilation-related hypocapnia) may be responsible for the low scaling exponents observed in patients with cardiovascular diseases (Dimopoulou et al., 2001; Johnson et al., 2000; Mazzara et al., 1974).

4.2. General conclusions and suggestions for further research

Our research calls for a reevaluation of fractal analysis of short-term HRV. As we have already noted, the use of scaling measures in physiological time series is interesting to the extent that it reveals information about the complex organization of underlining control mechanisms. Fractal long-term correlations in biological signals require the antagonistic interaction of nonlinearly coupled subsystems functioning and producing fluctuations at all scales (Struzik et al., 2004). At high frequencies, however, HRV is dominated by RSA, a well studied mechanism attributable to respiratory modulation of vagal efferent outflow to the heart (Denver et al., 2007; Grossman and Taylor, 2007). In addition, the time delays in sympathetic signal transduction caused by the intervention of second messenger cAMP for the depolarization of pacemaker cells in the sinoatrial node (Berntson et al., 1993; Levick, 2003), further support the notion that high-frequency HRV is driven by the parasympathetic system alone and is therefore not the right place to look for a substrate of complex nonlinear interactions.

This leads to the conclusion that DFA (and generally scaling analysis), is not valid when applied at small HRV scales. Alterations of the α_1 exponent by experimental manipulation or deviations from normal values in pathological populations cannot be attributed to a breakdown of fractal properties since those require a nonlinear coupling of multiple competing mechanisms functioning over a wide range of scales (Struzik et al., 2004). We suggest that a more detailed examination of breathing parameters and vagal cardiac influences would more adequately elucidate why the α_1 exponent is a good prognostic measure of various cardiovascular disorders.

Although we discourage the use of DFA for short-term HRV, we believe that it is a powerful algorithm to assess the correlation properties of cardiac IBI fluctuations at large scales. Ideally, long-term HRV scaling patterns are obtained by 24-h ECG recordings. Evidence suggests, however, that shorter data segments of approximately 8200 samples ($\approx$2-h recordings) do not significantly reduce the reliability of the DFA algorithm (Peng et al., 1995; Eke et al., 2002). This makes the use of DFA also suitable for behavioral experiments in laboratory settings.

The fractal $1/f$ noise observed in long-term HRV is also encountered in a certain class of physical systems which, for critical values of their parameters, exhibit complex organization characterized by long-term correlations among their individual components (Ivanov et al., 2004). In addition, Bak et al. have shown that for some physical systems, organization at a critical state with fractal geometries, scale invariance and power law long-term correlations, happens spontaneously without the need for any external adjustment of parameters (Bak, 1990). Bak used the term Self-Organizing Criticality (SOC) to describe this phenomenon which has been proposed as an explanation for fractal scale invariance in a wide variety of physical, biological and even social systems (Bak, 1996).

The characteristics of long-term correlations, scale invariance, and especially the absence of any fine tuning, make SOC an attractive principle to explain the dynamics of scale-free biological systems (Gisiger, 2001). The possibility of biological systems self-organizing in a critical state questions the traditional paradigm of homeostasis which postulates that in healthy organisms, physiologic control mechanisms operate to reduce variability generated by external perturbations in order to achieve an equilibrium-like state (Cannon, 1929). SOC, on the contrary, suggests that the goal of physiologic control may be to maintain a complex variability over a broad range of scales rather than a steady or periodic state, even in resting conditions (Goldberger, 1991).

The advantages of SOC have been mostly investigated in computer models. It has been shown that the capacity of scale-free networks to generate fluctuations at all scales optimizes information transmission (Beggs and Plenz, 2004; Bertschinger and Natschlager, 2004), and information storage by maximizing the number of repeating complex activation patterns (Haldeman and Beggs, 1998). Increased variability also allows a large number of different mappings between inputs and outputs which optimizes computational power without compromising the network's reliability (Latham and Nirenberg, 2004). Finally, fractal networks generate parallel trajectories in phase space, which means that despite increased variability, their dynamical evolution is still stable and controllable with minor corrective inputs (Bertschinger and Natschlager, 2004; Haldeman and Beggs, 1998). Remarkably, all these seemingly contradictory information processing tasks are optimized simultaneously when a system operates near the critical point (Beggs, 2008). Extrapolating the above results to cardiac dynamics, we can hypothesize that SOC in the cardiovascular system allows the heart to respond in a consistent manner to specific internal or external stimulation, while maintaining at the same time the flexibility to rapidly adjust to extreme perturbations.

The idea of complex variability is not new to psychophysiologists as the opposite extremes of strict periodicity (rigidity) and uncorrelated randomness are considered to contribute to inappropriate autonomic responses, characteristic of anxious and phobic patients (Friedman and Thayer, 1998; Friedman, 2007). In addition, there is a large amount of knowledge accumulated in the biopsychological literature regarding cardiac responsiveness to emotional and attentional stimuli. We believe that the application of new tools for the study of nonlinear dynamical systems may initiate a new line of psychophysiological research, where phasic cardiac responses to external stimuli can be used to test and support or reject the hypothesis of SOC in the cardiovascular system. In either case this will undoubtedly improve our understanding of how the various cardiac control mechanisms function as a whole in order to produce a fractal variability, and how this organization is disturbed in psychologically disordered states.

Acknowledgements

We would like to thank Gustavo Reyes del Paso and the anonymous reviewers of Biological Psychology for their valuable comments and suggestions that significantly improved the final version of this manuscript.

This work was supported by SEJ2004-07956 grant from the Spanish Ministry of Science and Innovation.

References

Allen, J., Chambers, A., Towers, D., 2007. The many metrics of cardiac chronotropy: a pragmatic primer and a brief comparison of metrics. Biological Psychology 74 (2), 243–262.
Bak, P., 1990. Self-organized criticality. Physica A 163 (1), 403–409.
Bak, P., 1996. How nature works: the science of self-organized criticality. Copernicus, New York.
Bak, P., Tang, C., Wiesenfeld, K., 1987. Self-organized criticality: an explanation of the $1/f$ noise. Physical Review Letters 59 (4), 381–384.
Beggs, J., 2008. The criticality hypothesis: how local cortical networks might optimize information processing. Philosophical Transactions of the Royal Society A 366 (1864), 329–343.
Beggs, J., Plenz, D., 2004. Neuronal avalanches are diverse and precise activity patterns that are stable for many hours in cortical slice cultures. Journal of Neuroscience 24 (22), 5216–5229.
Berntson, G., Cacioppo, J., Quigley, K., 1993. Respiratory sinus arrhythmia: autonomic origins, physiological mechanisms, and psychophysiological implications. Psychophysiology 30 (2), 183–196.
Berntson, G., Thomas Bigger, J., Eckberg, D., Grossman, P., Kaufmann, P., Malik, M., et al., 1997. Heart rate variability: origins, methods, and interpretive caveats. Psychophysiology 34 (6), 623–648.
Bertschinger, N., Natschlager, T., 2004. Real-time computation at the edge of chaos in recurrent neural networks. Neural Computation 16 (7), 1413–1436.
Boiten, F., Frijda, N., Wientjes, C., 1994. Emotions and respiratory patterns: review and critical analysis. International Journal of Psychophysiology 17 (2), 103–128.
Buldyrev, S., Dokholyan, N., Goldberger, A., Havlin, S., Peng, C., Stanley, H., et al., 1998. Analysis of DNA sequences using methods of statistical physics. Physica A 249 (1), 430–438.
Camm, A., Malik, M., Bigger Jr., J., et al., 1996. Heart rate variability: standards of measurement, physiological interpretation and clinical use. Task Force of the European Society of Cardiology and the North American Society of Pacing and Electrophysiology. Circulation 93, 1043–1065.
Cannon, W., 1929. Organization for physiological homeostasis. Physiological Reviews 9 (3), 399–431.
Carvalho, J., da Rocha, A., Nascimento, F., Souza Neto, J., Junqueira Jr., L., 2002. Development of a Matlab Software for Analysis of heart rate variability. Institute of Electrical and Electronics Engineers, Inc, Beijing, China.
Denver, J., Reed, S., Porges, S., 2007. Methodological issues in the quantification of respiratory sinus arrhythmia. Biological Psychology 74 (2), 286–294.
Dimopoulou, I., Tsintzas, O., Alivizatos, P., Tzelepis, G., 2001. Pattern of breathing during progressive exercise in chronic heart failure. International Journal of Cardiology 81 (2–3), 117–121.
Eke, A., Herman, P., Kocsis, L., Kozak, L., 2002. Fractal characterization of complexity in temporal physiological signals. Physiological Measurement 23 (1), 1–38.
Friedman, B., 2007. An autonomic flexibility–neurovisceral integration model of anxiety and cardiac vagal tone. Biological Psychology 74 (2), 185–199.
Friedman, B., Thayer, J., 1998. Anxiety and autonomic flexibility: a cardiovascular approach. Biological Psychology 47 (3), 243–263.
Gisiger, T., 2001. Scale invariance in biology: coincidence or footprint of a universal mechanism? Biological Reviews 76 (02), 161–209.
Goldberger, A., 1991. Is the normal heartbeat chaotic or homeostatic? Physiology 6 (2), 87–91.
Goldberger, A., Amaral, L., Glass, L., Hausdorff, J., Ivanov, P., Mark, R., et al., 2000. PhysioBank, PhysioToolkit, and PhysioNet: components of a new research resource for complex physiologic signals. Circulation 101 (23), 215–220.
Goldberger, A., Peng, C., Lipsitz, L., 2002. What is physiologic complexity and how does it change with aging and disease? Neurobiology of Aging 23, 23–26.
Grossman, P., Taylor, E.W., 2007. Toward understanding respiratory sinus arrhythmia: relations to cardiac vagal tone, evolution and biobehavioral functions. Biological Psychology 74 (2), 263–285.
Haldeman, C., Beggs, J., 1998. Critical branching captures activity in living neural networks and maximizes the number of metastable states. Physical Review Letters 94, 058101.
Hu, K., Ivanov, P., Chen, Z., Carpena, P., Stanley, H., 2001. Effect of trends on detrended fluctuation analysis. Physical Review E 64 (1), 011114–011119.
Huikuri, H., Mäkikallio, T., Peng, C., Goldberger, A., Hintze, U., Moller, M., 2000. Fractal correlation properties of RR interval dynamics and mortality in patients with depressed left ventricular function after an acute myocardial infarction. Circulation 101 (1), 47–53.
Huikuri, H., Mäkikallio, T., Perkiömäki, J., 2003. Measurement of heart rate variability by methods based on nonlinear dynamics. Journal of Electrocardiology 36, 95–99.
Ivanov, P., Chen, Z., Hu, K., Stanley, H., 2004. Multiscale aspects of cardiac control. Physica A 344 (3–4), 685–704.
Jensen, H., 1998. Self-organized Criticality: Emergent Complex Behavior in Physical and Biological Systems. Cambridge University Press, London.

Johnson, B., Beck, K., Olson, L., O'Malley, K., Allison, T., Squires, R., et al., 2000. Ventilatory constraints during exercise in patients with chronic heart failure. Chest 117 (2), 321–332.
Kantelhardt, J., Koscielny-Bunde, E., Rego, H., Havlin, S., Bunde, A., 2001. Detecting long-range correlations with detrended fluctuation analysis. Physica A 295 (3–4), 441–454.
Kleiger, R., Stein, P., Bigger, J., 2005. Heart rate variability: measurement and clinical utility. Annals of Noninvasive Electrocardiology 10 (1), 88–101.
Kobayashi, M., Musha, T., 1982. $1/f$ fluctuation of heartbeat period. IEEE Transactions on Biomedical Engineering 29 (6), 456–457.
Latham, P., Nirenberg, S., 2004. Computing and stability in cortical networks. Neural Computation 16 (7), 1385–1412.
Levick, J., 2003. An Introduction to Cardiovascular Physiology. Hodder Arnold, London.
Mahon, N., Hedman, A., Padula, M., Gang, Y., Savelieva, I., Waktare, J., et al., 2002. Fractal correlation properties of RR interval dynamics in asymptomatic relatives of patients with dilated cardiomyopathy. European Journal of Heart Failure 4 (2), 151–158.
Mandelbrot, B., 1983. The Fractal Geometry of Nature. WH Freeman, New York.
Mazzara, J., Ayres, S., Grace, W., 1974. Extreme hypocapnia in the critically ill patient. American Journal of Medicine 56 (4), 450–456.
Nagarajan, R., Kavasseri, R., 2005. Minimizing the effect of periodic and quasi-periodic trends in detrended fluctuation analysis. Chaos, Solitons and Fractals 26 (3), 777–784.
Peng, C., Buldyrev, S., Goldberger, A., Havlin, S., Sciortino, F., Simons, M., et al., 1992. Long-range correlations in nucleotide sequences. Nature 356, 168–170.
Peng, C., Havlin, S., Stanley, H., Goldberger, A., 1995. Quantification of scaling exponents and crossover phenomena in nonstationary heartbeat time series. Chaos: An Interdisciplinary Journal of Nonlinear Science 5, 82.
Peng, C., Mietus, J., Hausdorff, J., Havlin, S., Stanley, H., Goldberger, A., 1993. Long-range anticorrelations and non-gaussian behavior of the heartbeat. Physical Review Letters 70 (9), 1343–1346.
Penttila, J., Helminen, A., Jartti, T., Kuusela, T., Huikuri, H., Tulppo, M., et al., 2003. Effect of cardiac vagal outflow on complexity and fractal correlation properties of heart rate dynamics. Autonomic & Autacoid Pharmacology 23 (3), 173.
Perakakis, P., Guerra, P., Mata-Martin, J., Anllo-Vento, L., Vila, J., 2008. KARDIA: an open source graphic user interface for the analysis of cardiac interbeat intervals. Psychophysiology 45 (s1) addendum.
Saul, J., Albrecht, P., Berger, R., Cohen, R., 1988. Analysis of long term heart rate variability: methods, $1/f$ scaling and implications. Computers in Cardiology 14, 419–422.
Stam, C., Montez, T., Jones, B., Rombouts, S., van der Made, Y., Pijnenburg, Y., et al., 2005. Disturbed fluctuations of resting state EEG synchronization in Alzheimer's disease. Clinical Neurophysiology 116 (3), 708–715.
Stanley, H., Amaral, L., Buldyrev, S., Goldberger, A., Havlin, S., Leschhorn, H., et al., 1996. Scaling and universality in animate and inanimate systems. Physica A 231, 20–48.
Stanley, H., Amaral, L., Goldberger, A., Havlin, S., Ivanov, P., Peng, C., 1999. Statistical physics and physiology: monofractal and multifractal approaches. Physica A 270 (1–2), 309–324.
Stanley, H., Amaral, L., Gopikrishnan, P., Ivanov, P., Keitt, T., Plerou, V., 2000. Scale invariance and universality: organizing principles in complex systems. Physica A 281 (1–4), 60–68.
Stein, P., Barzilay, J., Chaves, P., Mistretta, S., Domitrovich, P., Gottdiener, J., et al., 2008. Novel measures of heart rate variability predict cardiovascular mortality in older adults independent of traditional cardiovascular risk factors: the cardiovascular health study (CHS). Journal of Cardiovascular Electrophysiology 19 (11), 1169–1174.
Struzik, Z., Hayano, J., Sakata, S., Kwak, S., Yamamoto, Y., 2004. $1/f$ scaling in heart rate requires antagonistic autonomic control. Physical Review E 70, 050901.
Vikman, S., Makikallio, T., Yli-Mayry, S., Pikkujamsa, S., Koivisto, A., Reinikainen, P., et al., 1999. Altered complexity and correlation properties of RR interval dynamics before the spontaneous onset of paroxysmal atrial fibrillation. Circulation 100 (20), 2079–2084.
Vjushin, D., Govindan, R., Brenner, S., Bunde, A., Havlin, S., Schellnhuber, H., 2002. Lack of scaling in global climate models. Journal of Physics Condensed Matter 14 (9), 2275–2282.
Voss, A., Schroeder, R., Truebner, S., Goernig, M., Figulla, H.R., Schirdewan, A., 2007. Comparison of nonlinear methods symbolic dynamics, detrended fluctuation, and Poincaré plot analysis in risk stratification in patients with dilated cardiomyopathy. Chaos: An Interdisciplinary Journal of Nonlinear Science 17, 015120.
Weron, R., 2002. Estimating long-range dependence: finite sample properties and confidence intervals. Physica A 312 (1–2), 285–299.
Xu, N., Shang, P., Kamae, S., 2008. Minimizing the effect of exponential trends in detrended fluctuation analysis. Chaos, Solitons and Fractals 41 (1), 311–316.